

Poly(lactic-co-glycolic acid) (PLGA) as Ion-Conducting Polymer for Biodegradable Light-Emitting Electrochemical Cells

Johannes Zimmermann,^{†,‡} Nils Jürgensen,^{†,‡} Anthony J. Morfa,^{†,‡} Bohui Wang,^{†,‡} Serpil Tekoglu,^{†,‡} and Gerardo Hernandez-Sosa^{*,†,‡}

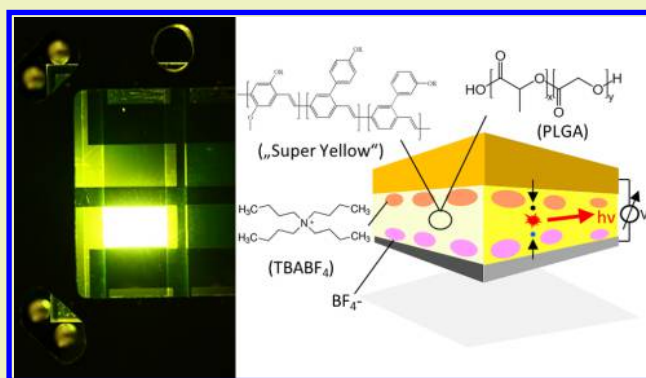
[†]Light Technology Institute, Karlsruhe Institute of Technology, Engesserstraße 13, 76131 Karlsruhe, Germany

[‡]InnovationLab, Speyererstraße 4, 69115 Heidelberg, Germany

S Supporting Information

ABSTRACT: The use of biocompatible and biodegradable materials in optoelectronics will enable the development of promising applications in the field of healthcare and environmental sensors as well as a more sustainable production of technology. Here, we present light-emitting electrochemical cells which utilize the biodegradable polymer poly(lactic-co-glycolic acid) (PLGA) to promote ionic conductivity in the active layer of light-emitting electrochemical cells. The device performance was analyzed in terms of the volume fraction of PLGA in the active layer blend as well as with respect to three different lactic:glycolic monomer ratios (85:15, 75:25, 65:35). In all three cases, adding PLGA to the active layer leads to an improvement of the turn-on voltage of up to 2 V compared to reference devices without PLGA. This can be attributed to an increase in ionic conductivity, which was determined by impedance spectroscopy. Increasing the relative amount of PLGA in the active layer shows that the improvement is ultimately limited by poor intermixing with the polymeric emitter as observed by fluorescent microscopy. The best devices achieved turn-on voltages of 4.1 V and a maximum luminance of 3800 cd m⁻² at 7.1 V.

KEYWORDS: Biopolymer, Biodegradable, Light-emitting electrochemical cell, Phase separation, Ion-conducting polymer, Solid polymer electrolyte



INTRODUCTION

Presently a large research effort is being made to investigate the use of biodegradable and biocompatible materials for electronic applications.^{1–4} These materials will enable the development of electronics that can be used in healthcare applications as well as in the sustainable production of green electronic devices.^{5–8} Materials such as silk, DNA, or *beta*-carotene have been successfully used as substrates or functional layers for the fabrication of electronic components such as transistors, OLEDs, or RF antennas.^{9–12} Conducting polymers like poly(styrenesulfonate) doped poly(dioxyethylenethiophene) (PEDOT:PSS) and poly(pyrrole) (PPy) show good biocompatibility and can be used as biocompatible electrode materials.^{3,13–16} Further development in this technological area has the potential to be used in applications that require a controlled degradation of electronic implants in the human body or potentially compostable electronics.^{17,18}

Poly(lactic-co-glycolic acid) (PLGA) is a commonly used material in medicine due to its biocompatibility. In the human body it undergoes nonenzymatic hydrolysis into nontoxic natural metabolites which are eliminated via the respiratory system.¹⁹ Accordingly it has granted the approval by the US

FDA for its use in clinical application.²⁰ PLGA is composed of lactic acid and glycolic acid monomer units where the corresponding ratio can be used to tune its degradation as well as its mechanical and chemical properties.²¹ The excellent characteristics of this material have enabled it to be used in drug delivery, tissue engineering, and modification of biological interfaces.^{22–26}

In this work, we investigate the application of PLGA as the ion-conducting polymer in solution-processed light-emitting electrochemical cells (LECs).^{27,28} Biomaterials such as agar, gelatin, poly(caprolactone), DNA, and starch have been used in the past for solid polymer electrolytes; however, none have been used in LECs.^{29–34} Figure 1 depicts the general working principle of a LEC device. The active layer consists of a light-emitting material that is mixed with an electrolyte. Applying a bias will lead to a separation of the cations and anions and a corresponding accumulation of charge at each electrode interface. This redistribution of ions will subsequently

Received: August 15, 2016

Revised: September 28, 2016

Published: September 29, 2016

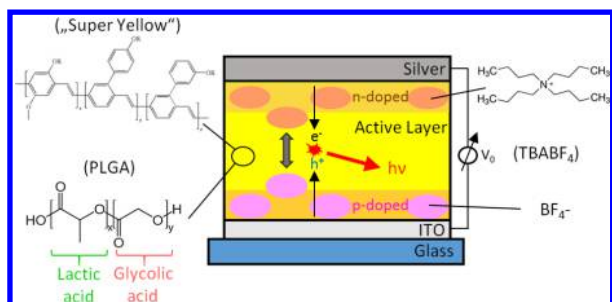


Figure 1. Working principle of a LEC device and chemical formulas of Super Yellow, PLGA, and TBABF₄.

contribute to the electrochemical doping of the semiconductor, dynamically forming n and p regions which will enable carrier injection from the electrodes for its subsequent recombination.³⁵ The intermixing of a conjugated light-emitting polymer and a polar electrolyte would be rather bad. Therefore, it is necessary for most devices to add an ion-conducting polymer to create pathways along which the ions can travel through the layer and to enable a better dissociation under device operation. This is in general caused by polar side chains of the respective polymer which are carbonyl groups in case of PLGA (Figure 1). The lactic acid monomer of PLGA has an additional CH₃ group making this part of the polymer more hydrophobic. Accordingly one can influence material properties by varying the monomer ratio, which should lead to differences in ionic conductivity and device morphology depending on the respective ratio.

Unlike organic light-emitting diodes (OLEDs), LECs do not require the deposition of charge injection/blocking interlayers. This simpler device architecture simplifies the fabrication process dramatically, especially in terms of industrially relevant printing processes.³⁶ Here we study the LEC performance as a function of monomer ratio and polymer fraction in the active layer to demonstrate that PLGA can be used in electronic devices which could open the path to the fabrication of fully biodegradable/biocompatible light-emitting devices.

EXPERIMENTAL SECTION

Materials. Super Yellow (SY, livlux PDY-132) was purchased from Merck. Poly(lactic-co-glycolic acid) (PLGA) and tetrabutylammonium tetrafluoroborate (TBABF₄) were purchased from Sigma-Aldrich. There are no studies about the biocompatibility of Super Yellow and TBABF₄ known to the authors. Three different blends of PLGA with 85:15, 75:25, and 65:35 lactic to glycolic monomer ratios have been used,

each with an average molecular weight of 63,000, 87,000, and 58,000 MW, respectively.

Device Fabrication. SY, PLGA, and TBABF₄ were dissolved separately in anisole at a concentration of 10 g L⁻¹ and stirred overnight. Afterward the materials were mixed together at the specific weight ratios and stirred for several hours. Then the solutions were spin-cast on prepatterned ITO (180 nm) coated glass substrates. To maintain a constant film thickness of ~120 nm, varying spin speeds between 1800 rpm and 1300 rpm for 45 s were used, followed by an additional drying step of 3500 rpm for 10 s. Subsequently the films were put into a vacuum oven for 2 h at 40 °C and 10 mbar to remove residual solvent. Top electrodes were produced by evaporating a 100 nm thick silver layer through a shadow mask. The area of the device active layer was 0.24 cm².

Cyclic Voltammetry. PLGA was dissolved in acetonitrile at a concentration of 20 g L⁻¹. Tetrabutylammonium hexafluorophosphate was used as a supporting electrolyte at a concentration of 0.1 M. The measurements were recorded using an Autolab PGSTAT302N potentiostat. The scan rate was set to 30 mV s⁻¹. All data shown is relative to a ferrocene reference (Fc/Fc⁺).

LIV/Lifetime Measurements. The electrical and optical characterization and the measurement of the lifetime were performed using a Botest characterization system. The light- and current-voltage (LIV) curves were recorded by sweeping the voltage with a rate of 100 mV s⁻¹ starting at 0 V. Lifetime measurements were performed at a constant current density of 42 mA cm⁻², pulsed at 1000 Hz with a duty cycle of 50%. The lifetime was defined as the time in which the luminance drops to half of its maximum value.

Ionic Conductivity Measurements. Data was recorded using an Autolab PGSTAT302N impedance analyzer. A Nyquist plot was recorded between 0.04 and 100,000 Hz at an amplitude of 50 mV. The data was fit to an equivalent circuit model (see Figures S1 and S2) to determine the ionic conductivity.³⁷

Fluorescent Microscopy. Fluorescence micrographs were taken with a Nikon DS-Filc fluorescent microscope. A halogen lamp with a blue band-pass filter of 465–495 nm was used as the excitation source. The emitted light was collected through a green band-pass filter (515–555 nm). Contrast and brightness of the pictures were adjusted afterward for better comparison.

Atomic Force Microscopy. Atomic force microscope (AFM) height profiles were taken in tapping mode at a resolution of 256 × 256 lines for 5 μm × 5 μm, using a DME DualScope 95-50 atomic force microscope.

Contact Angle. Measurements were performed using a Krüss DSA 100 drop shape analyzer.

RESULTS/DISCUSSION

In order to minimize detrimental chemical side reactions during device operation, it is necessary that the electrochemical stability window of the ion transporting polymer encompass both the oxidation and reduction potentials of the emitter

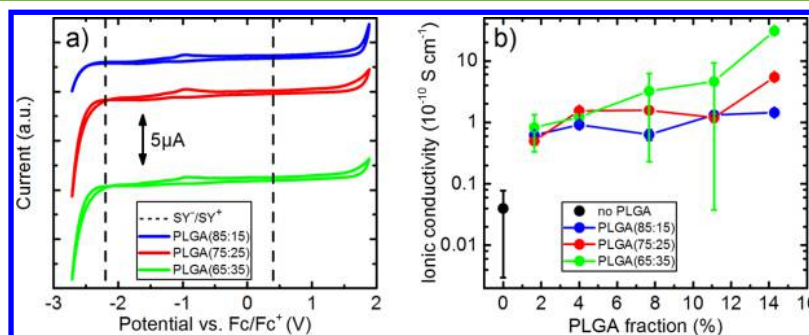


Figure 2. (a) Cyclic voltammetry measurements of PLGA for monomer ratios of 85:15, 75:25, and 65:35 vs ferrocene (Fc/Fc⁺). (b) Ionic conductivity of the device active layer, determined by impedance spectroscopy, and its dependence on monomer ratio in the PLGA, given in weight percent. The SY:TBABF₄ ratio is always 1:0.2.

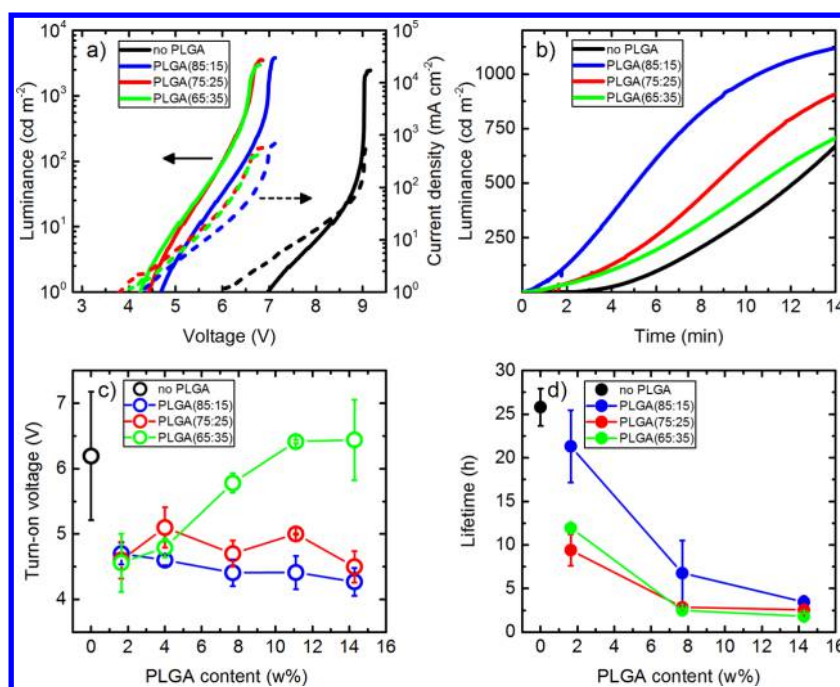


Figure 3. (a) LIV curves of devices built at a ratio of 1:0.02:0.2 (SY:PLGA:TBABF₄) for different monomer ratios. The black curve depicts a device without PLGA. (b) Corresponding turn-on time of the same devices as panel a at a constant bias of 4.5 V. Turn-on voltage (c) and lifetime (d) as a function of monomer ratio and the PLGA content given in wt %. The SY:TBABF₄ ratio is always 1:0.2.

material.³⁵ Figure 2a shows cyclic voltammetry measurements of PLGA with three different lactic:glycolic monomer ratios. In addition, the reduction and oxidation potentials of the emitting polymer, Super Yellow (SY), are depicted as vertical dashed lines.³⁶ Regardless of its monomer ratio, the irreversible reduction or oxidation of PLGA happens at larger potentials than that of the redox potentials of SY (−2.2 and 0.4 V, compared to ferrocene). This broader electrochemical stability window demonstrates the appropriateness of PLGA to be used as ion-conducting polymer for LECs in combination with SY. However, it is also visible that the onset of the oxidation potential of PLGA is lower for higher glycolic ratios, bringing it closer to the oxidation potential of the emitter material.

The realization of LEC devices that combine SY with a dissolved salt has been reported previously in the literature.^{36,38} However, due to the slow movement of ions through its polymer network, the addition of an ion-solvating polymer is required in order to achieve lower operational voltages and faster turn-on times of the devices.³⁵ These parameters are directly correlated to the ionic conductivity provided by the polyelectrolyte, which is in turn a function of its ion-solvating capabilities and film morphology.^{35,39} In this work, we initially fabricated LECs based on SY and TBABF₄ to determine the optimal mass ratio of 1:0.2, see Figure S3. Figure 2b shows the effect of the addition of PLGA on the ionic conductivity of the optimized SY:TBABF₄ system determined by impedance spectroscopy. We studied the three different lactic:glycolic monomer ratios, each at mass contents ranging from 0% to 14.2% relative to the emitter plus salt amount. In all cases, the addition of PLGA resulted in improved ionic conductivities. An increase of ~3 orders of magnitude was exhibited by the PLGA with the 65:35 monomer ratio at a fraction of 14% compared to the pristine SY:TBABF₄ sample which showed an ionic conductivity of 3×10^{-12} S cm⁻¹. The addition of PLGA with higher lactic monomer ratio resulted in a less pronounced

increase to values of $\sim 10^{-10}$ S cm⁻¹. These values are relatively low compared to previous works on polyelectrolytes based on biodegradable materials where ionic conductivities between 10^{-6} and 10^{-3} S cm⁻¹ are reported.^{32–34}

The increase of the ionic conductivity suggests that PLGA promotes ion movement within the film. This is demonstrated by the observed decrease in operational voltages shown in the luminance–current–voltage characteristics shown in Figure 3a. In LECs, the turn-on time is related to the time that the ions need to accumulate into doped regions at the contacts, enabling charge injection and subsequent recombination. Figure 3b presents the evolution of the luminance output of the devices during the first minutes of operation at a constant bias of 4.5 V. It is readily observed that the device without PLGA shows the slowest response due to having the lowest ionic conductivity of all samples. The turn-on speed of the samples containing PLGA correlates to the improvement of the ionic conductivity for low PLGA amounts (Figure 2b). Of the different monomer ratios used, 85:15 shows the fastest and 65:35 the slowest turn-on time. This is a consequence of different degradation rates for the respective monomer ratios as is depicted in Figure 3d. However, this cannot be differentiated in the ionic conductivity and LIV measurements because less current is used or the measurement is performed on a shorter time scale.

Compared to reference devices (containing only SY and TBABF₄), the addition of small amounts of PLGA (~1.6%) reduces the turn-on voltage (the voltage at which a luminance of 1 cd m⁻² is reached) by ~2 V. This trend occurs for all three monomer ratios to the same magnitude, and directly correlates to the behavior of the ionic conductivity determined by impedance spectroscopy (Figure 2b). However, the behavior of the turn-on voltage (Figure 3c) and the ionic conductivity differs, depending on the monomer ratio, when increasing PLGA content in the active layer. Particularly, for the PLGA 65:35, after initial decrease, an increase of the turn-on voltage is

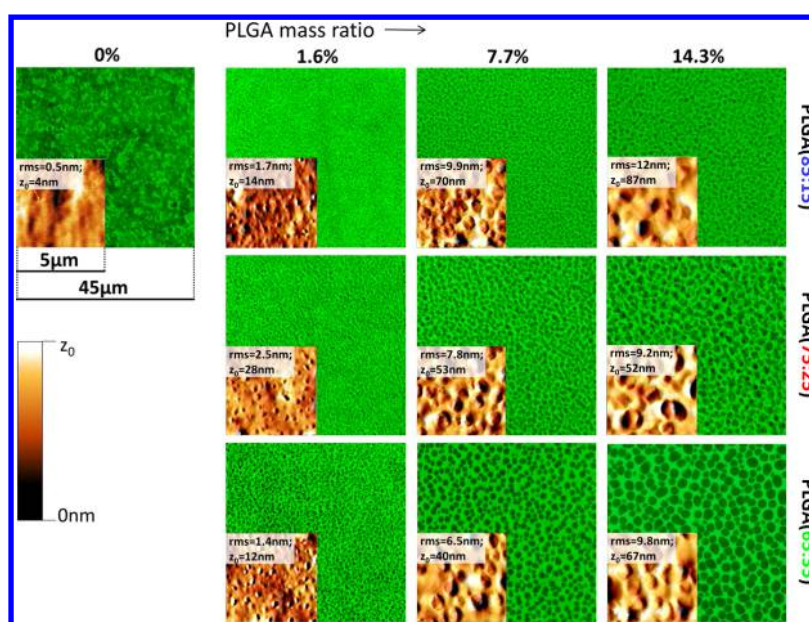


Figure 4. Fluorescent and atomic force micrographs demonstrating an increasing phase separation with PLGA content and the respective glycolic acid monomer ratio. The reference sample without PLGA shows a relatively inhomogeneous layer with SY rich and poor phases.

observed that reaches its initial value at $\sim 11\%$ PLGA fraction in spite of the increase in ionic conductivity. For the other monomer ratios the turn-on voltage exhibits the expected overall tendency to decrease with increasing PLGA fraction and larger ionic conductivity.

Figure 3d presents the device lifetime, defined as the time when the luminance drops by 50% of the maximum value. The operational lifetime in LECs is usually limited by adverse electrochemical reactions that take place during operation.^{40,41} The device with 1.6% PLGA with a monomer ratio of 85:15 shows the most stable properties compared to the other ratios. It has been reported in the literature that PLGA with a higher glycolic ratio is more prone to hydrolysis of the ester bond because of the increased water uptake that is a consequence of the stronger hydrophilicity.^{21,42} Indeed the cyclic voltammetry measurements in Figure 2a show a slightly smaller stability window for a monomer ratio of 85:15 compared to 75:25 and 65:35. Accordingly, the sample comprising the 85:15 monomer ratio PLGA exhibited lifetimes of over 20 h while the devices with 75:25 and 65:35 monomer ratios have lifetimes under 7 h. The lifetime of the device with no PLGA showed a slightly longer lifetime than the best PLGA containing sample. However, it shows higher operating voltages, slower turn-on dynamics, and consequently lower luminance at the same operating conditions due to the reduced mobility of TBABF₄. The complete lifetime measurements can be found in Figure S4.

In one of our previous studies we investigated the nonbiodegradable polymer poly(methyl-2-methylpropenoate) (PMMA) as ion-conducting polymer in combination with Super Yellow and TBABF₄ as well.³⁶ In this study turn-on voltages of only 8.5 V and lifetimes below 10 h were achieved for the best working devices, demonstrating that PLGA is a promising candidate for future applications.

Further insight into the device performance can be gained through the analysis of the film morphology. Figure 4 presents fluorescent (FM) and atomic force (AFM) micrographs of the LEC active layer at the concentrations discussed above as well as a reference sample without PLGA. PLGA and TBABF₄ do

not exhibit fluorescence in the spectral region of the chosen band-pass filter (515–555 nm), thus, the darker and brighter areas in the FM pictures represent SY poor and SY rich phases, respectively. The reference SY:TBABF₄ sample is shown in Figure 4; the SY emission is not homogeneous throughout the image due to the presence of TBABF₄ agglomerates. The addition of 1.6% PLGA qualitatively results in a more homogeneous light emission suggesting that PLGA promotes a better distribution of TBABF₄ in the active layer. This observation is supported by the higher ionic mobility and lower turn-on voltages shown in Figures 2 and 3. Overall, the system undergoes phase separation between SY and PLGA with increasing PLGA content. This can also be observed in the AFM measurements, with a commensurate increase in the root-mean-square roughness values. This trend is more pronounced if the PLGA has a higher glycolic monomer ratio. It has been reported that a higher glycolic monomer ratio in the PLGA polymer results in a more hydrophilic material showing water contact angles (θ_{water}) starting from 69° at a 50:50 monomer ratio up to 77° for 90:10.⁴³ This higher hydrophobicity would lead to poorer intermixing with the hydrophobic SY ($\theta_{\text{water}} = 94^\circ$) as observed in our experiments. The PLGA sample with a 65:35 monomer ratio exhibited an increased turn-on voltage in spite of the improved ionic conductivity. Based on the fluorescence images, we conclude that the higher ionic conductivity is exhibited in the PLGA rich phases, however, the observed phase separation does not favor electrochemical doping in the emitting material. This spontaneous phase separation ultimately limits device performance and highlights the importance of film micromorphology on device performance.³⁸

CONCLUSION

In summary, we demonstrated the use of the biodegradable PLGA as an ion-conductive polymer in LECs. The results make PLGA interesting for other applications besides its present use in drug delivery and tissue engineering. The device operation was observed to be influenced by the glycolic:lactic monomer

ratio of PLGA as well as the volume fraction in the active layer. The inclusion of PLGA increases ionic conductivity and decreases turn-on voltage compared to the SY:TBABF₄ reference. However, phase separation at higher PLGA volume fractions and larger glycolic:lactic ratios limits the improvement of the turn-on voltage. The best devices (which included 1.6% PLGA 85:15) exhibited operational lifetimes over 20 h with a turn-on voltage of 4.1 V and maximum luminance up to 3800 cd m⁻². For the development of fully biodegradable devices the salt and emitter need to be replaced by biocompatible substances. For this purpose the biodegradation of potential materials needs to be investigated. In order to improve the present device performance we suggest that further research focus on the development and modification of biodegradable polymers and the study of their biocompatibility.

■ ASSOCIATED CONTENT

📄 Supporting Information

The Supporting Information is available free of charge on the ACS Publications website at DOI: [10.1021/acssuschemeng.6b01953](https://doi.org/10.1021/acssuschemeng.6b01953).

Equivalent circuit models, detailed LIV characteristics, and lifetime measurements (PDF)

■ AUTHOR INFORMATION

Corresponding Author

*E-mail: gerardo.sosa@kit.edu.

Notes

The authors declare no competing financial interest.

■ ACKNOWLEDGMENTS

The authors acknowledge the support of the German Federal Ministry of Education and Research (BMBF) through Grant FKZ:03X5526.

■ REFERENCES

- (1) Mühl, S.; Beyer, B. Bio-Organic Electronics—Overview and Prospects for the Future. *Electronics* **2014**, *3*, 444–461.
- (2) Lanzani, G. Materials for Bioelectronics: Organic Electronics Meets Biology. *Nat. Mater.* **2014**, *13*, 775–776.
- (3) Berggren, M.; Richter-Dahlfors, A. Organic Bioelectronics. *Adv. Mater.* **2007**, *19*, 3201–3213.
- (4) Rivnay, J.; Owens, R. M.; Malliaras, G. G. The Rise of Organic Bioelectronics. *Chem. Mater.* **2014**, *26*, 679–685.
- (5) Svennersten, K.; Larsson, K. C.; Berggren, M.; Richter-Dahlfors, A. Organic Bioelectronics in Nanomedicine. *Biochim. Biophys. Acta, Gen. Subj.* **2011**, *1810*, 276–285.
- (6) Owens, R.; Kjall, P.; Richter-Dahlfors, A.; Cicoira, F. Organic Bioelectronics—Novel Applications in Biomedicine. Preface. *Biochim. Biophys. Acta, Gen. Subj.* **2013**, *1830*, 4283.
- (7) Irimia-Vladu, M.; Sariciftci, N. S.; Bauer, S. Exotic Materials for Bio-Organic Electronics. *J. Mater. Chem.* **2011**, *21*, 1350–1361.
- (8) Irimia-Vladu, M. “Green” Electronics: Biodegradable and Biocompatible Materials and Devices for Sustainable Future. *Chem. Soc. Rev.* **2014**, *43*, 588–610.
- (9) Kim, D.-H.; Kim, Y.-S.; Amsden, J.; Panilaitis, B.; Kaplan, D. L.; Omenetto, F. G.; Zakin, M. R.; Rogers, J. A. Silicon Electronics on Silk as a Path to Bioresorbable, Implantable Devices. *Appl. Phys. Lett.* **2009**, *95*, 133701.
- (10) Hwang, S.-W.; Huang, X.; Seo, J.-H.; Song, J.-K.; Kim, S.; Hage-Ali, S.; Chung, H.-J.; Tao, H.; Omenetto, F. G.; Ma, Z.; et al. Materials for Bioresorbable Radio Frequency Electronics. *Adv. Mater.* **2013**, *25*, 3526–3531.
- (11) Stadler, P.; Oppelt, K.; Singh, T. B.; Grote, J. G.; Schwödiauer, R.; Bauer, S.; Piglmayer-Brezina, H.; Bäuerle, D.; Sariciftci, N. S. Organic Field-Effect Transistors and Memory Elements Using Deoxyribonucleic Acid (DNA) Gate Dielectric. *Org. Electron.* **2007**, *8*, 648–654.
- (12) Hagen, J. A.; Li, W.; Steckl, A.; Grote, J. Enhanced Emission Efficiency in Organic Light-Emitting Diodes Using Deoxyribonucleic Acid Complex as an Electron Blocking Layer. *Appl. Phys. Lett.* **2006**, *88*, 171109.
- (13) Luo, S.-C.; Mohamed Ali, E.; Tansil, N. C.; Yu, H.; Gao, S.; Kantchev, E. A.; Ying, J. Y. Poly (3, 4-ethylenedioxythiophene) (PEDOT) Nanobiointerfaces: Thin, Ultrasoft, and Functionalized PEDOT Films with in Vitro and in Vivo Biocompatibility. *Langmuir* **2008**, *24*, 8071–8077.
- (14) Kim, Y. H.; Lee, J.; Hofmann, S.; Gather, M. C.; Müller-Meskamp, L.; Leo, K. Achieving High Efficiency and Improved Stability in ITO-Free Transparent Organic Light-Emitting Diodes with Conductive Polymer Electrodes. *Adv. Funct. Mater.* **2013**, *23*, 3763–3769.
- (15) Balint, R.; Cassidy, N. J.; Cartmell, S. H. Conductive Polymers: Towards a Smart Biomaterial for Tissue Engineering. *Acta Biomater.* **2014**, *10*, 2341–2353.
- (16) Onoda, M.; Abe, Y.; Tada, K.; Kawakita, Y.; Fujisato, T.; Uto, S. Conductive Polymers as Bioelectronic Materials. *Electronics and Communications in Japan* **2013**, *96*, 24–31.
- (17) Acar, H.; Çinar, S.; Thunga, M.; Kessler, M. R.; Hashemi, N.; Montazami, R. Study of Physically Transient Insulating Materials as a Potential Platform for Transient Electronics and Bioelectronics. *Adv. Funct. Mater.* **2014**, *24*, 4135–4143.
- (18) Hwang, S.-W.; Song, J.-K.; Huang, X.; Cheng, H.; Kang, S.-K.; Kim, B. H.; Kim, J.-H.; Yu, S.; Huang, Y.; Rogers, J. A. High-Performance Biodegradable/Transient Electronics on Biodegradable Polymers. *Adv. Mater.* **2014**, *26*, 3905–3911.
- (19) Gilding, D. Biodegradable Polymers. In *Biocompatibility of clinical implant materials*; Williams, D. F., Ed.; CRC Press: Boca Raton, 1981; Vol. 2, pp 209–232.
- (20) Lü, J.-M.; Wang, X.; Marin-Muller, C.; Wang, H.; Lin, P. H.; Yao, Q.; Chen, C. Current Advances in Research and Clinical Applications of PLGA-Based Nanotechnology. *Expert Rev. Mol. Diagn.* **2009**, *9*, 325.
- (21) Anderson, J. M.; Shive, M. S. Biodegradation and Biocompatibility of PLA and PLGA Microspheres. *Adv. Drug Delivery Rev.* **2012**, *64*, 72–82.
- (22) Makadia, H. K.; Siegel, S. J. Poly Lactic-Co-Glycolic Acid (PLGA) as Biodegradable Controlled Drug Delivery Carrier. *Polymers (Basel, Switz.)* **2011**, *3*, 1377–1397.
- (23) Fredenberg, S.; Wahlgren, M.; Reslow, M.; Axelsson, A. The Mechanisms of Drug Release in Poly (lactic-Co-Glycolic Acid)-Based Drug Delivery Systems—a Review. *Int. J. Pharm.* **2011**, *415*, 34–52.
- (24) Nair, L. S.; Laurencin, C. T. Biodegradable Polymers as Biomaterials. *Prog. Polym. Sci.* **2007**, *32*, 762–798.
- (25) Dhandayuthapani, B.; Yoshida, Y.; Maekawa, T.; Kumar, D. S. Polymeric Scaffolds in Tissue Engineering Application: A Review. *Int. J. Polym. Sci.* **2011**, *2011*, 1.
- (26) Gentile, P.; Chiono, V.; Carmagnola, I.; Hatton, P. V. An Overview of Poly (lactic-Co-Glycolic) Acid (PLGA)-Based Biomaterials for Bone Tissue Engineering. *Int. J. Mol. Sci.* **2014**, *15*, 3640–3659.
- (27) Costa, R. D.; Ortí, E.; Bolink, H. J. Recent Advances in Light-Emitting Electrochemical Cells. *Pure Appl. Chem.* **2011**, *83*, 2115–2128.
- (28) Pei, Q.; Yu, G.; Zhang, C.; Yang, Y.; Heeger, A. J. Polymer Light-Emitting Electrochemical Cells. *Science* **1995**, *269*, 1086–1088.
- (29) Leones, R.; Sentanin, F.; Rodrigues, L.; Marrucho, I.; Esperança, J.; Pawlicka, A.; Silva, M. Investigation of Polymer Electrolytes Based on Agar and Ionic Liquids. *eXPRESS Polym. Lett.* **2012**, *6*, 1007.
- (30) Anderson, C. F.; Record, M. T., Jr. Polyelectrolyte Theories and Their Applications to DNA. *Annu. Rev. Phys. Chem.* **1982**, *33*, 191–222.

- (31) Kumar, M.; Tiwari, T.; Srivastava, N. Electrical Transport Behaviour of Bio-Polymer Electrolyte System: Potato Starch+ Ammonium Iodide. *Carbohydr. Polym.* **2012**, *88*, 54–60.
- (32) Lopes, L.; Dragunski, D.; Pawlicka, A.; Donoso, J. Nuclear Magnetic Resonance and Conductivity Study of Starch Based Polymer Electrolytes. *Electrochim. Acta* **2003**, *48*, 2021–2027.
- (33) Vieira, D. F.; Avellaneda, C. O.; Pawlicka, A. Conductivity Study of a Gelatin-Based Polymer Electrolyte. *Electrochim. Acta* **2007**, *53*, 1404–1408.
- (34) Fonseca, C. P.; Rosa, D. S.; Gaboardi, F.; Neves, S. Development of a Biodegradable Polymer Electrolyte for Rechargeable Batteries. *J. Power Sources* **2006**, *155*, 381–384.
- (35) Mindemark, J.; Edman, L. Illuminating the Electrolyte in Light-Emitting Electrochemical Cells. *J. Mater. Chem. C* **2016**, *4*, 420–432.
- (36) Hernandez-Sosa, G.; Tekoglu, S.; Stolz, S.; Eckstein, R.; Teusch, C.; Trapp, J.; Lemmer, U.; Hamburger, M.; Mechau, N. The Compromises of Printing Organic Electronics: A Case Study of Gravure-Printed Light-Emitting Electrochemical Cells. *Adv. Mater.* **2014**, *26*, 3235–3240.
- (37) Huggins, R. Simple Method to Determine Electronic and Ionic Components of the Conductivity in Mixed Conductors a Review. *Ionics* **2002**, *8*, 300–313.
- (38) Shao, Y.; Bazan, G. C.; Heeger, A. J. Long-Lifetime Polymer Light-Emitting Electrochemical Cells. *Adv. Mater.* **2007**, *19*, 365.
- (39) Tang, S.; Edman, L. Quest for an Appropriate Electrolyte for High-Performance Light-Emitting Electrochemical Cells. *J. Phys. Chem. Lett.* **2010**, *1*, 2727–2732.
- (40) Shin, J. H.; Matyba, P.; Robinson, N. D.; Edman, L. The Influence of Electrodes on the Performance of Light-Emitting Electrochemical Cells. *Electrochim. Acta* **2007**, *52*, 6456–6462.
- (41) Fang, J.; Matyba, P.; Edman, L. The Design and Realization of Flexible, Long-Lived Light-Emitting Electrochemical Cells. *Adv. Funct. Mater.* **2009**, *19*, 2671–2676.
- (42) Park, T. G. Degradation of Poly (lactic-Co-Glycolic Acid) Microspheres: Effect of Copolymer Composition. *Biomaterials* **1995**, *16*, 1123–1130.
- (43) Norris, D. A.; Puri, N.; Labib, M. E.; Sinko, P. J. Determining the Absolute Surface Hydrophobicity of Microparticulates Using Thin Layer Wicking. *J. Controlled Release* **1999**, *59*, 173–185.